CENTER FOR CONNECTED AND AUTOMATED TRANSPORTATION

Final Report #ICT-23-017
August 2023

Artificial Intelligence for Optimal Truck Platooning: Impact on Autonomous Freight Delivery

Tong Liu
Hadi Meidani

ILLINOIS CENTER FOR TRANSPORTATION

DISCLAIMER

Funding for this research was provided by the Center for Connected and Automated Transportation under Grant No. 69A3551747105 of the U.S. Department of Transportation, Office of the Assistant Secretary for Research and Technology (OST-R), University Transportation Centers Program. The contents of this report reflect the views of the authors, who are responsible for the facts and the accuracy of the information presented herein. This document is disseminated under the sponsorship of the Department of Transportation, University Transportation Centers Program, in the interest of information exchange. The U.S. Government assumes no liability for the contents or use thereof.

Suggested APA Format Citation:

Liu, T., & Meidani, H. (2023). *Artificial intelligence for optimal truck platooning: Impact on autonomous freight delivery* (Report No. ICT-23-017). Illinois Center for Transportation. https://doi.org/10.36501/0197-9191/23-017

Contacts

For more information:

Hadi Meidani
University of Illinois Urbana-Champaign
1211 Newmark Civil Engineering Bldg
meidani@illinois.edu
https://ict.illinois.edu

CCAT
University of Michigan Transportation Research Institute
2901 Baxter Road
Ann Arbor, MI 48152
uumtri-ccat@umich.edu
(734) 763-2498
www.ccat.umtri.umich.edu

TECHNICAL REPORT DOCUMENTATION PAGE

1. Report No.	2. Government Accession No.	3. Recipient's Catalog No.
ICT-23-017	N/A	N/A

4. Title and Subtitle	5. Report Date
Artificial Intelligence for Optimal Truck Platooning: Impact on Autonomous Freight Delivery	August 2023
	6. Performing Organization Code N/A

7. Authors	8. Performing Organization Report No.
Tong Liu (https://orcid.org/0000-0002-3667-917X) and Hadi Meidani (https://orcid.org/0000-0003-4651-2696)	ICT-23-017 UILU-ENG-2023-2017

9. Performing Organization Name and Address	10. Work Unit No.
Illinois Center for Transportation Department of Civil and Environmental Engineering University of Illinois at Urbana-Champaign 205 North Mathews Avenue, MC-250 Urbana, IL 61801	N/A
	11. Contract or Grant No. Grant No. 69A3551747105

12. Sponsoring Agency Name and Address	13. Type of Report and Period Covered
Center for Connected and Automated Transportation University of Michigan Transportation Research Institute 2901 Baxter Road Ann Arbor, MI 48152	Final Report
	14. Sponsoring Agency Code

15. Supplementary Notes

Funding under Grant No. 69A3551747105 U.S. Department of Transportation, Office of the Assistant Secretary for Research and Technology (OST-R), University Transportation Centers Program.
https://doi.org/10.36501/0197-9191/23-017

16. Abstract

The advancements in autonomous- and connected-vehicle technologies bring drastic changes in freight delivery. Vehicle-to-vehicle and vehicle-to-infrastructure communication has become a reality with the help of autonomous and connected vehicles. One of the most notable changes is the formation of truck platoons. Despite the numerous benefits of truck platooning, such as reduced fuel consumption and increased traffic efficiency, this approach requires a significant amount of computational resources to obtain aerodynamic performance under different scenarios. To overcome this challenge, a data-driven surrogate model was proposed to predict the drag force and fuel-consumption rate of truck platoons. The surrogate model improves computational efficiency, as compared to traditional methods, and provides a valuable tool for evaluating the performance of truck platoons. To demonstrate the benefits of truck platooning, a 161-km (100-mi) corridor in Illinois on I-57 highway was selected to conduct fuel-consumption analysis and delivery-cost analysis for a three-truck platoon. The results showed that the average fuel savings achieved can be up to 10%, depending on the headway between the trucks. The delivery cost of the truck platoon was reduced by 30%, as compared with conventional line-haul delivery. These findings highlighted the importance of truck platooning as a solution for reducing fuel consumption and improving delivery economy in the freight industry.

17. Key Words	18. Distribution Statement
Truck Platooning, Freight Delivery, Fuel Consumption, Artificial Neural Network, Surrogate Modeling, Aerodynamics	No restrictions. This document is available through the National Technical Information Service, Springfield, VA 22161.

19. Security Classif. (of this report)	20. Security Classif. (of this page)	21. No. of Pages	22. Price
Unclassified	Unclassified	28	N/A

ACKNOWLEDGMENT, DISCLAIMER, MANUFACTURERS' NAMES

This project was conducted in cooperation with the Center for Connected and Automated Transportation and the Illinois Center for Transportation. The contents of this report reflect the view of the authors, who are responsible for the facts and the accuracy of the data presented herein. The contents do not necessarily reflect the official views or policies of CCAT or ICT. This report does not constitute a standard, specification, or regulation. Trademark or manufacturers' names appear in this report only because they are considered essential to the object of this document and do not constitute an endorsement of the product by CCAT or ICT.

EXECUTIVE SUMMARY

The emergence of autonomous and connected trucks (ACTs) has introduced significant changes in freight delivery, impacting efficiency, safety, energy consumption, and infrastructure durability. One important change is the formation of truck platoons, made feasible and practical by the intelligent technologies integrated into ACTs. Although truck platooning has benefits in fuel consumption and traffic efficiency, it requires substantial computational resources to optimize the aerodynamic performance of the platoon. To overcome these challenges, data-driven surrogate models were developed that significantly improved computational efficiency. We compared the performance of the data-driven surrogate model to baseline models that included linear regression and support-vector regression. The results demonstrated the effectiveness of surrogate models for drag-force prediction and highlight their potentials for real-time applications in truck platoons.

Furthermore, a fuel-consumption and cost-analysis of truck freight delivery was conducted as case study. The real wind speed and direction data was collected from a wind station close to the corridor. The length of the corridor was 161 km (100 mi), with high platoonability. The wind history along the highway segment was collected, and delivery windows were chosen based on fluctuations in wind speed and direction. The study demonstrated the potential for truck platooning to reduce fuel consumption. Additionally, by automating truck delivery, the fuel consumption for truck operation and the required number of truck drivers are reduced, which made the bulk of the operational cost less than the conventional delivery scheme. The cost-benefit analysis of truck-platoon-based delivery indicated that truck-platoon technology can reduce the delivery cost, as compared with conventional truck delivery.

TABLE OF CONTENTS

CHAPTER 1: INTRODUCTION 1

OVERVIEW 1

OBJECTIVES 9

CHAPTER 2: AERODYNAMIC ANALYSIS OF A TRUCK PLATOON 10

WIND-DATA COLLECTION 10

TRUCK-PLATOON AERODYNAMICS 11

TRUCK-PLATOON GEOMETRY AND MESH FORMULATION 14

DRAG-FORCE AND FUEL-CONSUMPTION ANALYSIS 15

CHAPTER 3: DATA-DRIVEN SURROGATE MODEL FOR DRAG-FORCE PREDICTION OF A THREE-TRUCK PLATOON 17

GENERALIZED ADDITIVE MODEL 17

ARTIFICIAL NEURAL NETWORK 18

EXPERIMENT SETUP 19

EXPERIMENT RESULT 20

CHAPTER 4: ARTIFICIAL INTELLIGENCE FOR CONNECTED-TRUCK FREIGHT DELIVERY: A CASE STUDY 21

CASE STUDY SETUP 21

SUMMARY 25

REFERENCES 26

LIST OF FIGURES

Figure 1. Graph. Fuel saving of field measurements, as compared with wind tunnel tests. 3
Figure 2. Graph. Flow-velocity curves at 10% truck share and various equipment rates with CACC. 3
Figure 3. Flowchart. Truck modeling, sensor reading, information passing, and control system. 4
Figure 4. Photos. Configuration of automated platoon of 3 heavy trucks and a light truck. 5
Figure 5. Graph. Estimated fuel savings in leading and trailing vehicles, averaged over three different yaw angles. 5
Figure 6. Photo. Truck platoon model in wind tunnel. 6
Figure 7. Graph. Effect of separation and offset distances on wind-averaged-drag-coefficient reduction of the two-truck platoon. 6
Figure 8. Graph. Average fuel-reduction ratio as a function of the distance gap for a three-truck platoon. 7
Figure 9. Chart. The correlation matrix between variables impacting fuel consumption. 8
Figure 10. Graph. Annual wind rose plot for Rantoul, Illinois. 10
Figure 11. Graph. Annual wind rose plot for Peoria, Illinois. 11
Figure 12. Diagram. Schematic illustration of truck platooning, side view. 12
Figure 13. Diagram. Schematic illustration of truck platooning, top view. 12
Figure 14. Equation. Mass-conservation equation. 13
Figure 15. Equation. Fluid-momentum equation. 13
Figure 16. Equation. Turbulent kinetic energy equation. 13
Figure 17. Equation. Dissipation-rate equation. 13
Figure 18. Diagram. Computational domain of a three-truck platoons. 14
Figure 19. Diagram. Mesh generation of truck platoon, side view. 14
Figure 20. Diagram. Mesh generation around truck, side view. 15
Figure 21. Diagram. Mesh generation around truck, cross-section view. 15
Figure 22. Equation. Drag-coefficient calculation. 15
Figure 23. Equation. Resistance load of the truck-platooning system. 16
Figure 24. Equation. Estimated fuel cost due to aerodynamics force. 16
Figure 25. Equation. Estimated fuel cost due to pavement roughness. 16
Figure 26. Equation. Estimated fuel-consumption-reduction ratio. 16

Figure 27. Equation. Link function for the generalized additive model. 17
Figure 28. Equation. Iteratively backfitting in the generalized additive model. 18
Figure 29. Equation. Restricted-maximum-likelihood estimation. 18
Figure 30. Equation. Single layer of a fully connected network. 18
Figure 31. Equation. Mean-square error. 19
Figure 32. Map. Map of the highway corridor in Illinois. 21
Figure 33. Graph. Wind history along the highway corridor. 22
Figure 34. Graphs. Average drag-force prediction under various headways 23
Figure 35. Graph. Fuel-consumption-reduction ratio for a three-truck platoon. 24
Figure 36. Graph. Delivery-cost comparison between three-truck platoon and nonplatoon. 24

LIST OF TABLES

Table 1. Performance Comparison of Various Surrogate Models 20

CHAPTER 1: INTRODUCTION

OVERVIEW

The transportation system sector is considered one of the critical infrastructure systems, as designated by the Cybersecurity and Infrastructure Security Agency, US Department of Homeland Security. However, increasing travel and delivery demands create a burden on the transportation system and lead to severe issues such as traffic congestion, accidents, and environmental pollution. To address these challenges, technological developments have been introduced in the transportation industry. Intelligent transportation systems (ITS) have emerged as a promising future direction to alleviate the issues by integrating a range of systems, including sensing, communication, information dissemination, and traffic control. This futuristic plan has enabled the communication of vehicles, infrastructures, smartphones, and other devices. Over the last two decades, ITS has proven to be an effective way of improving the performance of transportation systems, enhancing travel security, and providing more choices to travelers.

In recent years, the field of ITS has experienced a significant transformation due to the availability of additional data. This data availability has revolutionized ITS development, with a growing emphasis on data-intensive and data-driven approaches (Zhang et al., 2011b). For instance, computer-vision-based technologies have been widely implemented in many ITS applications, including road-sign recognition (Khan et al., 2010), pedestrian counting (Zhang et al., 2011a), vehicle-plate recognition (Pustokhina et al., 2020), traffic control (Van der Pol and Oliehoek, 2016), and autonomous vehicles (Bounini et al., 2015). Furthermore, different types of sensors are used in ITS, including global positioning systems, laser radars, and ultrasound detectors. A global positioning system is frequently used in ITS to track vehicle trajectories in real time. However, its performance may need to be improved in scenarios involving high-rise buildings and tunnels. To address this issue, Schleicher et al. (2009) proposed a data-fusion approach that incorporates vision data with global positioning system data as a complementary source. In another study, Gidel et al. (2010) utilized a multilayer laser scanner mounted at the front of vehicles to detect pedestrian positions. In addition to the aforementioned aspects, the availability and integration of data related to human factors, vehicles, and infrastructures are crucial in enhancing transportation equity in conjunction with the development of intelligent transportation systems. By leveraging advanced analytics and modeling techniques, transportation stakeholders can analyze the collected data and develop evidence-based strategies to mitigate disparities and improve equity in transportation services and infrastructure (Liu and Meidani, 2023).

The data exchange in ITS can be grouped into four categories (Dar et al., 2010): vehicle-to-vehicle (V2V), vehicle-to-infrastructure (V2I), pedestrian-to-infrastructure (P2I), and vehicle-to-pedestrian (V2P). V2V is the ability to exchange spatial and temporal information about surrounding vehicles wirelessly. It shows great promise to avoid traffic accidents, mitigate traffic congestion, and improve environmental quality. V2I refers to a communication framework that enables vehicles to exchange information with transportation-infrastructure systems through various devices. V2V and V2I require a reliable data-transmission system with low latency and high accuracy (Dar et al., 2010). To guarantee the quality of service, high capacity, and ultrareliability of V2V links, Zhao et al. (2020)

maximized the total capacity of V2I links while guaranteeing the strict transmission delay and reliability constraints of V2V links using a multi-agent, double deep Q-learning algorithm. In recent years, casualties from pedestrian accidents caused by vehicles have been increasing. P2I and V2P communication is proposed to increase pedestrian and vehicle safety by establishing direct communication between vehicles and pedestrians. Liu et al. (2018) dealt with a cooperative system of V2I/P2I communication with radar perception at an intersection. The radar detects these vehicles or pedestrians and sends their position information to other vehicles or pedestrians.

From the perspective of energy consumption, the transportation-system sector is the second most significant global energy sector. By 2016, road-freight vehicles consumed 17 million barrels of oil per day. Moreover, the demand growth in road freight outpaced that of all other sectors. It is expected to be increased by a factor of 2.4 by the year of 2050 (Teter, 2017). In the road-transportation sector, the heavy-duty vehicle (HDT) is a non-negligible source of fuel consumption. Schroten et al. (2012) indicate that 5% of total energy consumption comes from HDTs. Many attempts have been made to reduce this high and growing fuel-consumption demand in the road-freight industry to improve fuel efficiency. Gong et al. (2010) proposed an approximate model and optimization approach of the aerodynamic shape of a container truck's wind deflector to minimize the drag coefficient of the container truck. Moreover, truck-platooning technology was proposed at the intersection of the ITS and the road-freight vehicle. The idea of truck platooning is to place trucks one after another within a close distance by using ACT technology. Truck platooning will become more feasible and practical with the intelligent technologies existing in the ACT that enable the connection among vehicles and between vehicles and infrastructure. While the safe headway for human-driven trucks is 50 m (165 ft) in Europe and 60 m (200 ft) in the United States, enabling communication technologies embedded in ACTs can reduce this distance to 3 m (10 ft) in a truck platoon (Browand et al., 2004).

Truck platooning has become an increasingly popular solution for reducing energy consumption in the freight industry. One of the primary sources of truck fuel consumption and emissions is aerodynamic drag force. This drag is caused by the pressure difference between the high-pressure zone in the front of a truck and the low-pressure zone in the rear. In a platoon, the trailing trucks benefit from reduced pressure drag because the leading trucks block the air, which lowers the pressure in the frontal zone. Leading trucks also benefit from reduced aerodynamic drag because the trailing trucks compress the turbulent flow, increasing the pressure in the low-pressure zone. To analyze fuel consumption for truck platooning, researchers commonly use three main methods: wind tunnel tests, road tests, and computational fluid dynamics (CFD) simulations. Wind tunnel tests are useful for studying isolated components of the platoon, such as the truck's drag coefficient but may not accurately represent the complex flow patterns found on the road. Road tests provide more realistic data but can be expensive. CFD simulations are time-consuming but cost-effective and provide detailed information on the platoon's aerodynamic performance, making them a popular choice for evaluating platoon configurations and optimizing fuel consumption.

Browand (2004) conducted a field experiment on fuel consumption of a two-truck platoon with truck headway of 3 to 10 m, in which the trucks were interconnected by means of an electronic control system. The experiments were performed on an unused airfield runway at Crows Landing, California. The main length of the runway was 2,400 m. The fuel-saving result from field data was also compared

with wind tunnel experiment, as shown in Figure 1. The measured fuel consumption at a spacing of 10 m for leading truck and trailing truck was 6% and 10%, respectively.

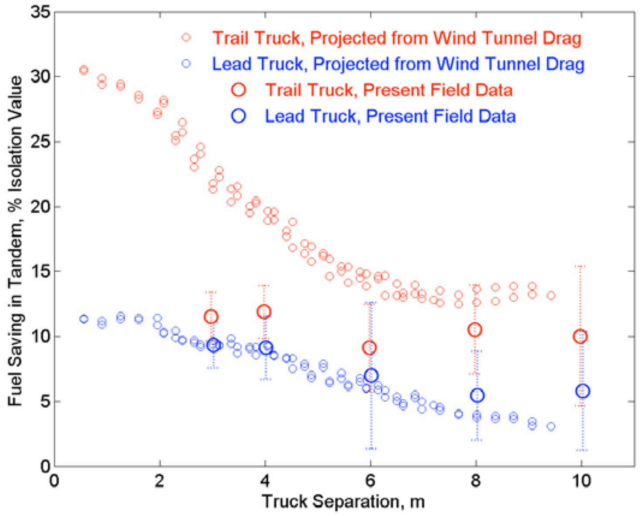

Figure 1. Graph. Fuel saving of field measurements, as compared with wind tunnel tests.

Source: Browand, 2004

Furthermore, another benefit of truck platooning is to increase road capacity to provide more room for surrounding traffic with the help of cooperative adaptive cruise control (CACC) technology. In the CACC-equipped, truck-platooning system, the leading truck is operated by driver and the following truck can be fully automated. Müller (2012) modelled CACC-equipped truck platoons in VISSIM, where the length of the experiment track is 3.1 mi (5000m). Three categories of vehicles (passenger cars, light trucks, and HDTs) were considered in the simulated environment. The vehicle velocity in Figure 2 indicated that CACC-equipped trucks on traffic flow for a three-lane highway can increase the road capacity and average vehicle speed by 5.5% and 6.4%, respectively.

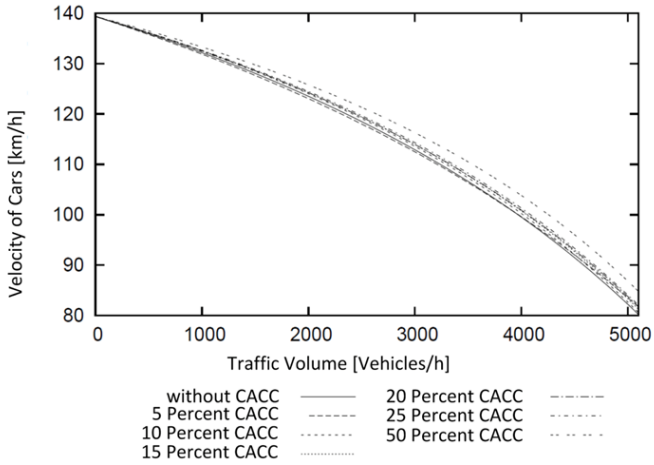

Figure 2. Graph. Flow-velocity curves at 10% truck share and various equipment rates with CACC.

Source: Müller, 2012

Lu and Shladover (2014) conducted experiments on coordinated, automatic, longitudinal control of a three-truck platoon. The figure 3 shows the control system, sensor reading, and information passing of the truck system. Furthermore, the platoon system was tested with constant-speed, acceleration, and deceleration cruising conditions using dedicated short-range communication coordination. Additionally, headway between the trucks was controlled between 4 m (13.1 ft) and 10 m (32.7 ft) to evaluate the effects of aerodynamic drag reductions on fuel savings. The experiments' result indicated that at the 6-m (19.6-ft) gap, fuel savings of lead truck and following truck is about 4% to 5% and 10% to 14 %, respectively.

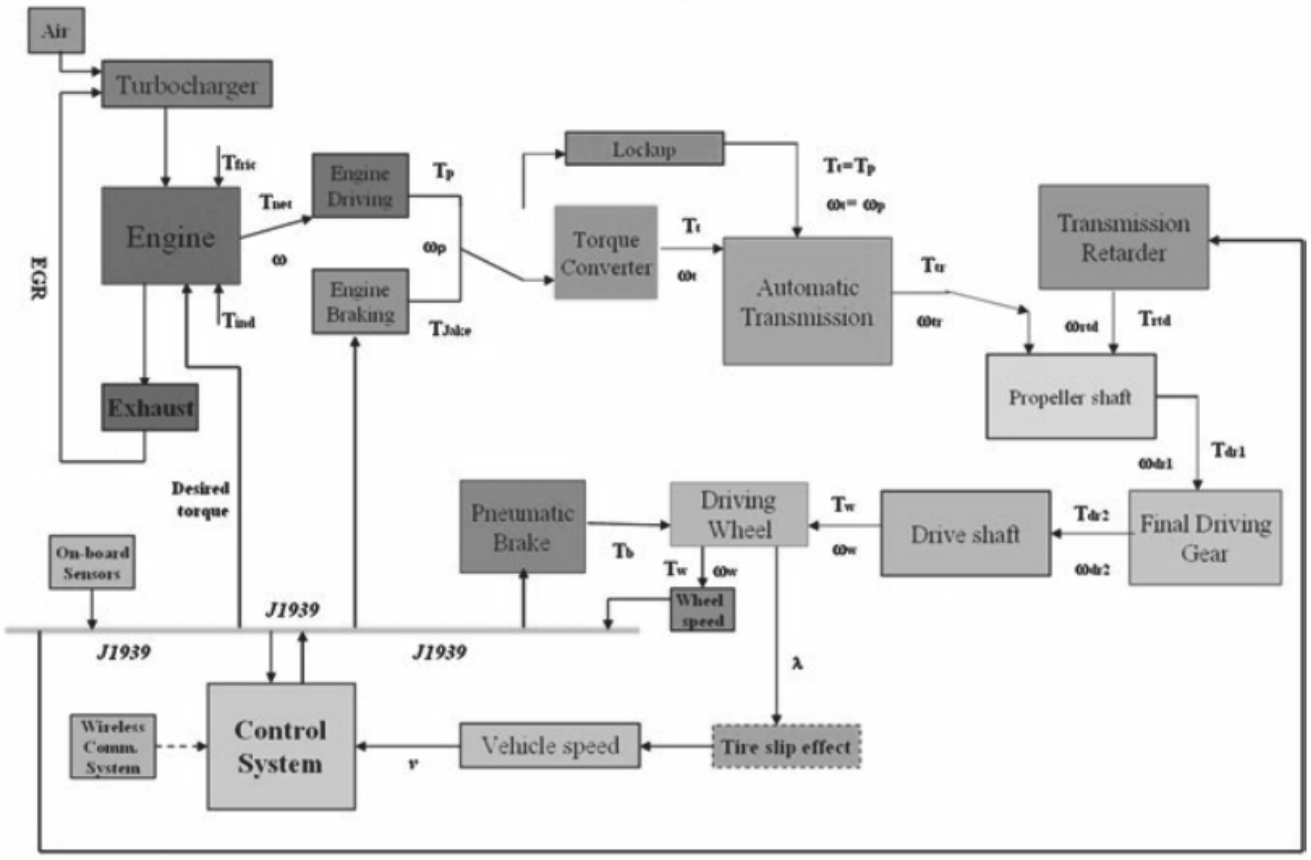

Figure 1. Flowchart. Truck modeling, sensor reading, information passing, and control system.

Source: Lu and Shadier, 2014

Tsugawa (2014) presented an automated truck-platoon system within a national ITS project named "Energy ITS" A platoon of three trucks drove at 80 km/h (50 mph) with the headway of up to 4.7 m (15.4 ft). Figure 4 shows the field test configuration of the truck platoons, including three heavy trucks and one light truck. The lateral offset of the platoon was controlled with lane-marker detection by computer vision. Also, the longitudinal headway was controlled by 76-GHz radar and LiDAR, in addition to the inter-vehicle communications of 5.8-GHz, dedicated short-range communication and infrared.

Figure 4. Photos. Configuration of automated platoon of 3 heavy trucks and a light truck.

Source: Tsugawa, 2014

Vegendla et al. (2015) studied the impact of platooning on aerodynamic characteristics, which was investigated through three-dimensional modeling and numerical simulations using the CFD simulation. The study analyzed five different platooning configurations to gain insight into their effects. The CFD simulation employed the k-ε turbulence model to model gas-phase turbulence and considered a computational domain of 200 m × 500 m × 200 m to capture the vortex at the trailer's rear. Results in Figure 5 indicated that the fuel-consumption-reduction benefit decreased as the separation distance between leading and trailing vehicles increased. This observation was noted for both leading and trailing vehicles.

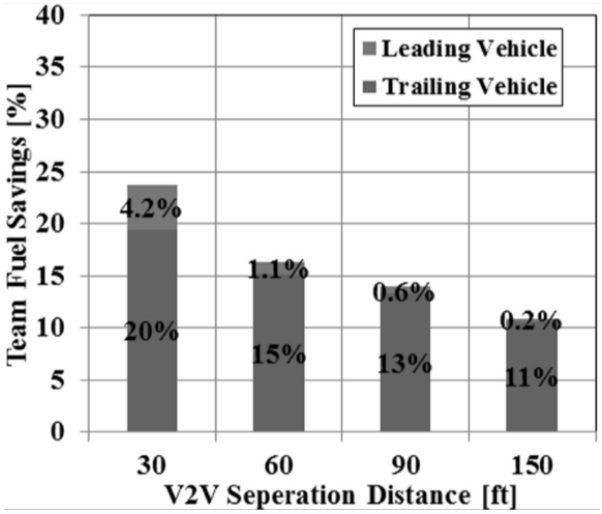

Figure 5. Graph. Estimated fuel savings in leading and trailing vehicles, averaged over three different yaw angles.

Source: Vegendla et al., 2015

Humphreys and Bevly (2016) investigated the impact of the separation distance on fuel consumption in a driver-assistive, truck-platooning system. The researchers conducted multiple experiments with different headways to analyze the relationship between headway and drag reduction. The results showed that the performance of the truck platoon improved as the headway decreased, indicating

that closer spacing between the trucks led to greater drag reduction and increased fuel efficiency. Additionally, the study found that the exchange of information between trucks not only improved fuel economy but also increased safety.

McAuliffe and Ahmadi-Baloutaki (2018) conducted a wind tunnel study to investigate the drag-reduction potential in two-truck platooning of different factors that may influence fuel saving and greenhouse gas reduction. As shown in Figure 6, the experiments were undertaken in a wind tunnel with two aerodynamic tractors of 1/15-scale models paired with dry-van trailers. In addition, to estimate the air inflow, a pressure probe was mounted on the trailing model. The experiments observed that all platoon cases achieved a reduction in wind-averaged-drag coefficient, as compared with their performance in isolation. The averaged drag reduction of the two-truck platooning system decreased when separation distance, i.e., headway, increased. As shown in Figure 7, increasing the offset distance from 0 to 0.15 and 0.31 model widths did not significantly affect the drag reduction of the platoon unit.

Figure 6. Photo. Truck platoon model in wind tunnel.

Source: McAuliffe and Ahmadi-Baloutaki, 2018

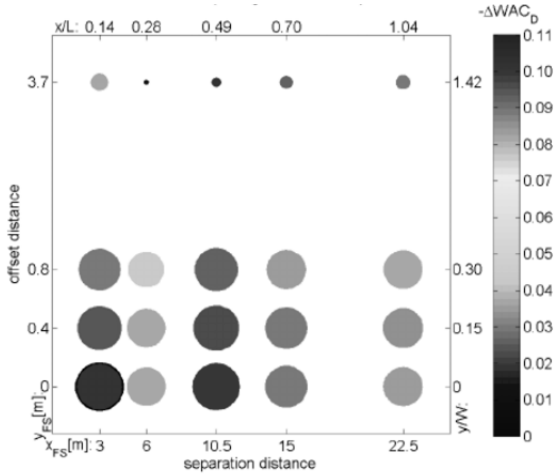

Figure 7. Graph. Effect of separation and offset distances on wind-averaged-drag-coefficient reduction of the two-truck platoon.

Source: McAuliffe and Ahmadi-Baloutaki, 2018

Hussein and Rakha (2021) presented a comprehensive model that characterizes the influence of inter-vehicle headway and offset on the drag coefficient of a platoon system of different vehicles. The study analyzed the fuel savings that could be achieved by using homogeneous platoons of light-duty vehicles, buses, and HDTs to quantify the potential reduction in fuel consumption beyond existing empirical measurements. The authors utilized rational polynomials to develop models that capture the impact of offset and headway on the drag coefficient. The fuel reduction ratio in Figure 8 shows that the fuel savings achieved by bus and HDT platoons are comparable, indicating that using HDT drag coefficients for buses was more reliable. These findings provide essential insights into the potential benefits of platooning and can help to guide future efforts aimed at improving the energy efficiency of vehicle fleets. By reducing fuel consumption, platooning has the potential to significantly reduce greenhouse gas emissions and improve sustainability in the transportation sector.

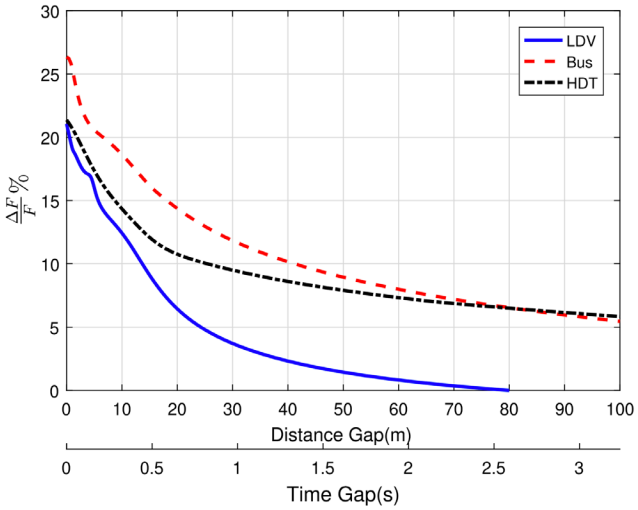

Figure 8. Graph. Average fuel-reduction ratio as a function of the distance gap for a three-truck platoon.

Source: Hussein and Rakha, 2021

Along with the development of artificial intelligence and machine learning, the data-driven approach has been extensively applied in ITS ecosystems (Mak et al., 2018). Machine-learning algorithms are being used in various applications. To illustrate, these methods leverage the availability of large datasets to learn the underlying features and patterns hidden within the data, allowing for accurate predictions and insights. By employing machine learning techniques, data-driven methods can transform raw data into a latent space representation, where the essential features and relationships are captured. This latent space representation enables efficient and effective predictions based on learned patterns and correlations. Consequently, data-driven methods have the potential to revolutionize various fields by providing valuable insights, optimizing processes, and enabling informed decision-making based on knowledge learned from the data. The neural network has shown its ability and potential in different areas, including computer vision (Ho et al., 2019), natural language processing (Wan et al., 2020), and graph modeling (Liu and Meidani, 2022). The data-driven approaches can be categorized into supervised learning, unsupervised learning, and reinforcement-learning approaches. Supervised learning maps from input space into a corresponding output space,

which requires labeled data and output in the training process. Unsupervised learning performs a similar task as the supervised learning approach but without any labeled information. Reinforcement learning enables an agent to learn in an interactive environment by receiving rewards, using feedback from its actions through the Markov decision process. The machine learning approach has been used for estimating the fuel consumption and greenhouse gas emission (Khurana 2021) of HDTs. Furthermore, Katreddi and Thiruvengadam (2021) implemented a fully connected neural network to model fuel consumption in HDTs for predicting the total and instantaneous fuel consumption of a trip. The parameters considered in the neural networks are engine load, engine speed, and vehicle speed; trip distance; fuel temperature; and actual torque. The correlation analysis in Figure 9 indicated that the accelerator-pedal position, actual torque, power, and engine load are highly correlated to each other, with a correlation coefficient of 0.85 and higher.

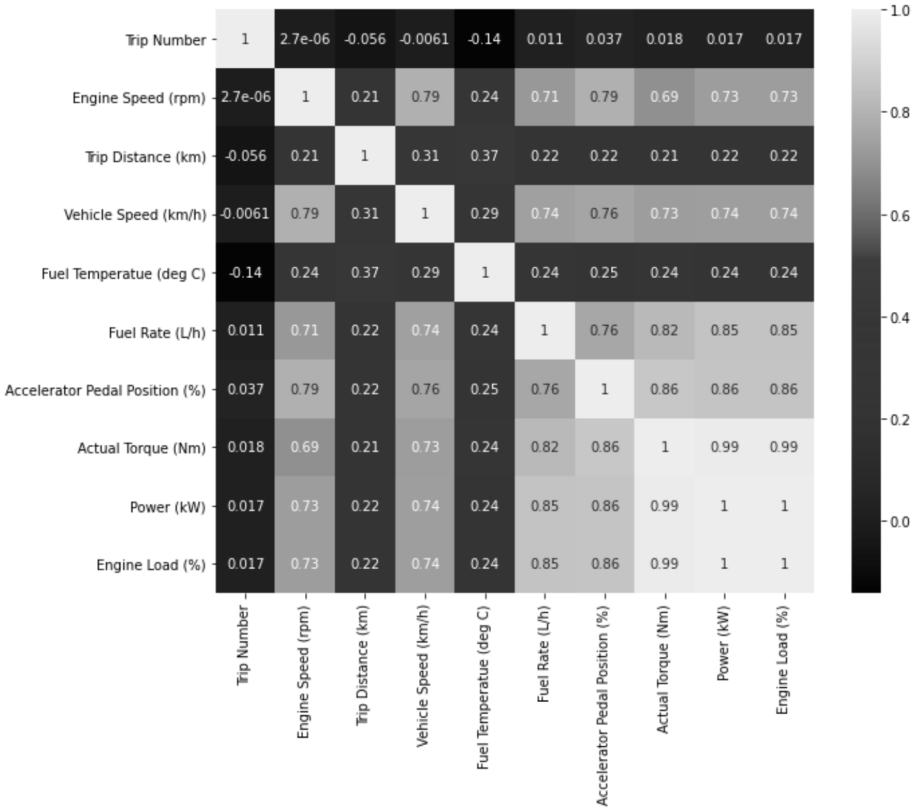

Figure 9. Chart. The correlation matrix between variables impacting fuel consumption.

Source: Katreddi and Thiruvengadam, 2021

The aforementioned approaches, however, ignore the fuel-saving performance under different wind conditions (wind speed, wind direction). It is not fully investigated due to the high computational time of CFD simulation. Additionally, to reduce fuel consumption, the truck platoon needs to be reconfigured because the wind speed and wind direction changes during the trip. Therefore, it is essential to develop a data-driven approach to build a surrogate model for drag-force prediction under different wind conditions. The surrogate model can be used to optimize the truck configuration

to maximize fuel savings under different scenarios. In addition, the surrogate model can also be integrated into a decision-making system to reconfigure the truck platoon during the trip based on real-time wind data. This approach can significantly reduce the computational time and cost required for fuel-saving analysis and optimization of HDTs, while also contributing to the reduction of greenhouse gas emissions.

OBJECTIVES

The main objective of this study is to quantify and predict the drag force and fuel consumption of truck platooning under various wind scenarios and truck configurations. In addition, based on the surrogate model, this study also determines the optimal platoon to minimize fuel consumption under different scenarios. Also, this study uses a real scenario to showcase the economic potential and implication of truck platooning for the delivery industry. The major tasks will be completed in the following order:

1. Build the finite-element model for drag-force prediction and fuel-consumption analysis under different wind scenarios. Formulate the surrogate model for rapid drag-force prediction and compare the prediction performance of different models.

2. Use the pretrained surrogate model to determine the optimal platooning configuration to minimize fuel consumption under different wind scenarios.

3. Conduct cost-benefit analysis for a three-truck platoon and compare the delivery cost of truck-platoon-based delivery with conventional truck delivery. To demonstrate the benefits of truck platooning, a 160-km (100-mile) corridor in Illinois on I-57 highway was selected to conduct fuel-consumption analysis and delivery-cost analysis on a three-truck platoon.

CHAPTER 2: AERODYNAMIC ANALYSIS OF A TRUCK PLATOON

WIND-DATA COLLECTION

To accurately consider the impact of wind on fuel reduction in a truck-platooning system, it is essential to collect wind-data history, including wind-speed and wind-direction history. The wind-history data in the local area is crucial for evaluating the impact of wind on fuel consumption on local routes. These data typically include wind speed, wind direction, and temperature. To collect these data, wind stations are set up at different locations; and wind-data history with 20-minute resolution is available and collected. Furthermore, these data can be summarized through the wind rose plot to provide a graphical representation of the wind data, which is useful in evaluating the impact of wind on fuel consumption. The plot consists of a circular diagram divided into segments, with each segment representing a different wind direction. The length of the segments corresponds to the frequency or intensity of the wind coming from that direction. The wind speed data is typically represented by color-coding or shading within each segment, with darker colors indicating higher wind speeds. Figure 10 and Figure 11 present the annual wind rose plot at Rantoul, Illinois, and Peoria, Illinois, respectively, which are collected from (Iowa State University, 2023) . It is clearly indicated that the pattern difference of wind speed and direction distribution could be distinguishable at different locations.

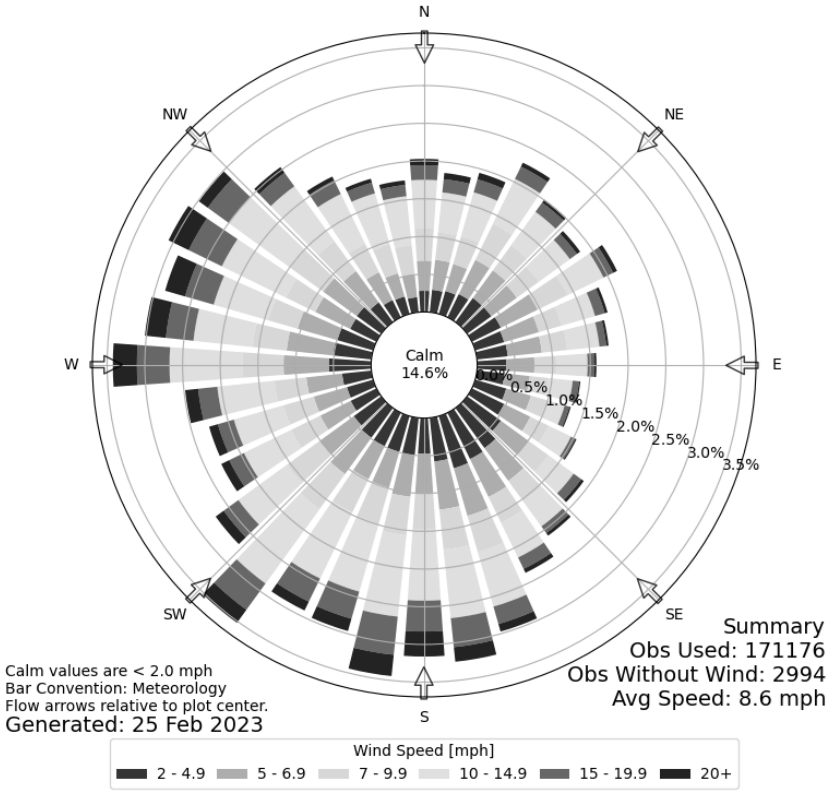

Figure 10. Graph. Annual wind rose plot for Rantoul, Illinois.

Source: Iowa State University, 2023

Furthermore, to obtain more detailed and accurate wind measurements from the truck side, it is possible to collect wind data close to the truck surface using an ultrasonic anemometer (McAuliffe et al., 2017). This device is mounted on the truck and provides real-time wind speed and direction data. Compared with the weather-station data, the truck-side ultrasonic anemometer data could reflect the wind condition around the truck more accurately. However, in the case where no external instrument is available for truck-side measurement, the wind-station data can be used. In this report, we used the weather-station data for the CFD simulation.

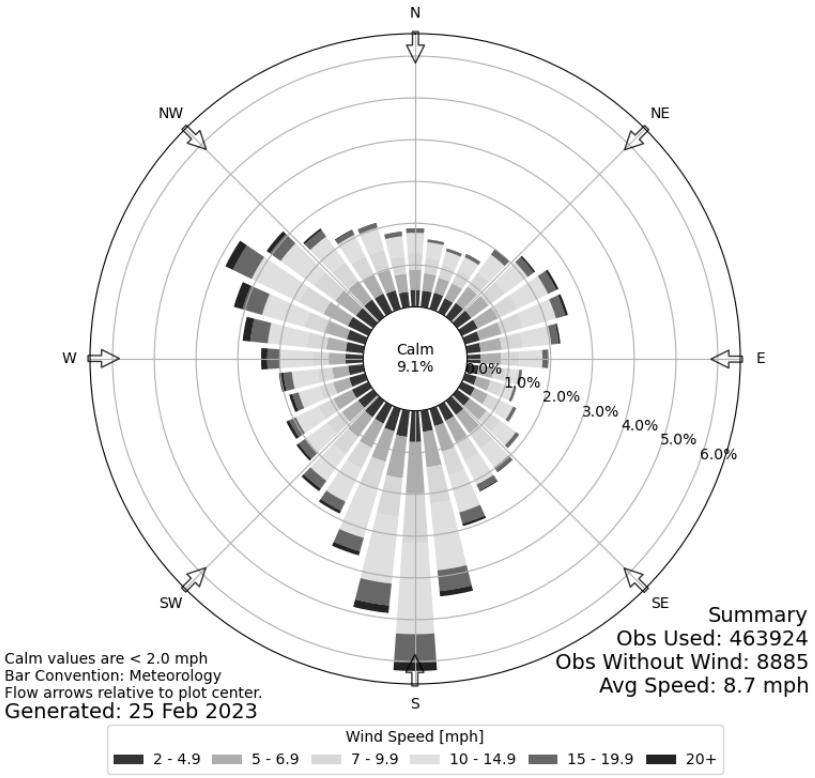

Figure 11. Graph. Annual wind rose plot for Peoria, Illinois.

Source: Iowa State University, 2023

Additionally, fuel-consumption analysis of truck platoons can be analyzed in the short and long term. For short-term analysis, the fuel consumption will be calculated based on a one-day trip, given the wind condition. For the long-term analysis, the fuel-consumption reduction will be calculated based on the frequency of wind occurrence from the wind rose plot, which will be achieved through Monte Carlo simulation from the wind rose plot. The wind data will be used for surrogate modeling to estimate the drag coefficient and fuel-consumption rate, which are discussed in the following sections.

TRUCK-PLATOON AERODYNAMICS

The aerodynamic drag of a truck is a major factor that affects its fuel-consumption rate. This drag force is caused by the pressure difference between the front and rear of the truck, in which the front

is a high-pressure zone and the rear is a low-pressure zone. In truck platooning, the drag force on each truck is reduced, resulting in a decrease in fuel consumption. The reason for this reduction in drag force is that trailing trucks experience a decrease in pressure drag, which lowers the pressure in the frontal zone. For leading trucks, the aerodynamic drag decreases because the trailing truck compresses the turbulent flow, which increases the pressure in the low-pressure zone. This phenomenon has been observed and demonstrated through multiple experiments, including wind tunnel tests (McAuliffe and Ahmadi-Baloutaki, 2018) and numerical simulations (Vegendla et al., 2015). The extent of drag reduction is affected by various factors such as the truck geometry, the relative position of adjacent vehicles, and external environmental factors. When the spacing between trucks increases, the drag-reduction effect is mitigated. External factors such as truck geometry, wind speed, and wind direction also impact the drag-reduction performance, as the pressure zone for each truck changes. In this study, the drag-reduction performance of truck-platooning system is simulated as a function of headway, offset, and wind condition using Ansys Fluent (ANSYS, Inc., 2016). The schematic views of the truck platooning system are presented in Figure 12 and Figure 13.

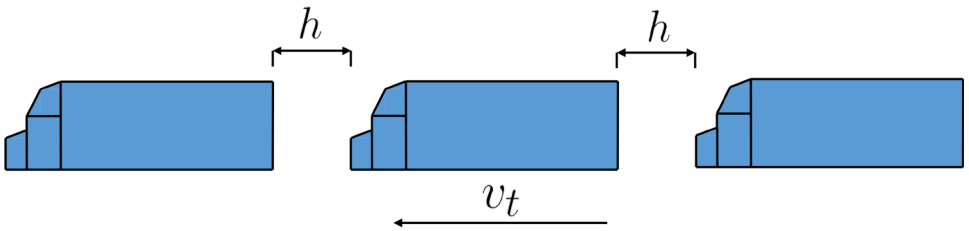

Figure 12. Diagram. Schematic illustration of truck platooning, side view.

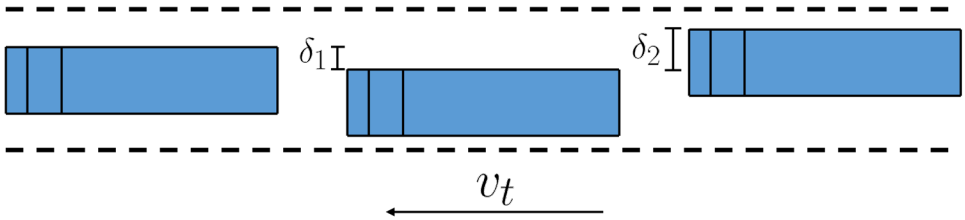

Figure 13. Diagram. Schematic illustration of truck platooning, top view.

To solve the complex aerodynamic problems of a truck-platooning system, it is necessary to set up controlling equations for truck aerodynamics. Reynolds-averaged Navier-Stokes equations are chosen as the governing equations to simulate the turbulent flow. Reynolds-averaged Navier-Stokes equations differ from Navier-Stokes equations in that they account for the effects of turbulence, using Reynolds averaging. This technique involves averaging the velocity and pressure fields over a small interval, which effectively separates the mean flow from the fluctuating flow. The flow of fluid is described by three basic conservation laws: mass conservation, momentum conservation, and energy conservation. The mass-conservation equation is a fundamental equation in fluid mechanics that describes the conservation of mass in a fluid system. It states that the rate of change of mass within a control volume must equal the net rate of mass flow into or out of the control volume. The mass-conservation equation is presented in Figure 14:

$$\frac{\partial \rho}{\partial t} + \nabla \cdot \{\rho \boldsymbol{u}\} = 0$$

Figure 14. Equation. Mass-conservation equation.

Where ρ is the fluid density, and $\boldsymbol{u}$ is the velocity vector of fluid at time t. The momentum equation expresses the law of conservation of momentum for moving fluid. The rate of change of total momentum of any micro unit in a flow field is equal to the resultant force of all external forces acting on the micro unit. The expression of the fluid momentum equation is as shown in Figure 15:

$$\frac{\partial(\rho \boldsymbol{u})}{\partial t} + \nabla \cdot \{\rho \boldsymbol{u}\boldsymbol{u}^T\} = -\nabla p + \nabla \cdot \{\mu \nabla \boldsymbol{u}\} + \rho \boldsymbol{g} - \frac{1}{3}\rho \nabla \cdot \boldsymbol{u}\boldsymbol{I} + \boldsymbol{R}$$

Figure 15. Equation. Fluid-momentum equation.

Where p is the pressure, μ is the dynamic viscosity, $\boldsymbol{g}$ is the gravitational acceleration vector, $\boldsymbol{I}$ is the identity tensor, and $\boldsymbol{R}$ is the Reynolds stress tensor. To solve the Reynolds-averaged Navier-Stokes equations, a turbulence model must be used to close the equations, which provides closure for the Reynolds stresses. In this model, the k-epsilon model is used as the turbulence model. The k-epsilon turbulence model adds two equations to the system. The turbulent kinetic energy k is modeled mathematically as shown in Figure 16:

$$\frac{\partial \rho k}{\partial t} + \nabla \cdot (\rho k \boldsymbol{u}) = \nabla \cdot (\frac{\mu_t}{\sigma_k} \nabla k) - 2\rho\epsilon$$

Figure 16. Equation. Turbulent kinetic energy equation.

Where μ_t is the turbulent viscosity, σ_k is the turbulent Prandtl number for k, ϵ is the dissipation rate due to molecular viscosity, and $\rho\epsilon$ is the viscous dissipation term. The dissipation rate ε is expressed as shown in Figure 17:

$$\frac{\partial(\rho\epsilon)}{\partial t} + \nabla \cdot (\rho\epsilon \boldsymbol{u}) = \nabla \cdot (\frac{\mu_t}{\sigma_\epsilon} \nabla \epsilon) + C_{1\epsilon}\frac{\epsilon}{k} 2\rho\epsilon - C_{2\epsilon}\frac{\epsilon^2}{k}$$

Figure 17. Equation. Dissipation-rate equation.

Where $\sigma_\epsilon$is the turbulent Prandtl number for ϵ. $C_{1\epsilon}$ and $C_{2\epsilon}$ are constants, and the last two terms on the right-hand side represent production and destruction of turbulence, respectively. The turbulence-model equations require additional closure relationships for the turbulent viscosity μ_t, the turbulent Prandtl numbers σ_k and σ_ϵ, and the constants $C_{1\epsilon}$ and $C_{2\epsilon}$. These closures are typically based on empirical correlations and must be calibrated for specific flow conditions.

TRUCK-PLATOON GEOMETRY AND MESH FORMULATION

Due to the lack of open-source commonly used truck models, the drag force of the truck platooning is simulated over modified Ahmed bodies (Liu and Moser, 2003), including an inclined surface to simulate aerodynamic characteristics of the common semitrailer truck. The input parameters include the truck geometry, truck configuration (speed v_t, headway h, and offset δ), and wind configuration (wind speed v_w and wind direction). The truck is assumed to be a heavy-duty truck; and the truck weight is adopted from (McAuliffe et al., 2017), which is 29,500 kg (65,000 lb). The type of the aerodynamic flow is air, and the temperature and density are 25° C and 0.0765 lb/ft^3, respectively. To simulate the aerodynamics of the truck-platoon system, a larger computational domain is built to cover the truck-platoon system. The geometry of the truck platoon and computational domain is presented in Figure 18.

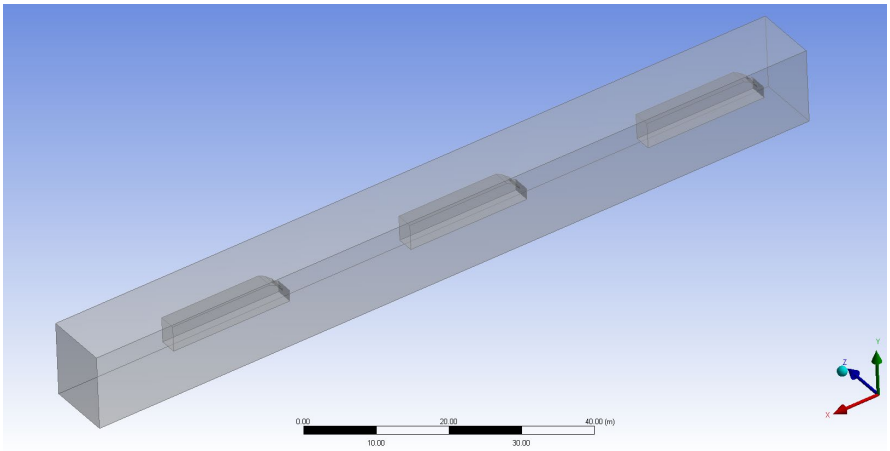

Figure 18. Diagram. Computational domain of a three-truck platoons.

The mesh-generation process is an important step to obtain accurate and reliable results for the numerical simulations. To ensure a high-quality mesh, several parameters were carefully selected. The grid resolution and feature size were chosen as 0.1 m (4 in.) and 0.001 m (0.04 in.), respectively, to ensure an appropriate level of detail for the complex flow field around the truck platoon. In addition, a five-layer inflation layer was added with a growth rate of 1.2 and a transition ratio of 0.72. These inflation layers were defined on the surfaces of interest, including the truck surfaces and road surfaces, to improve mesh quality and capture the boundary-layer effects. Moreover, refinement boxes were defined in regions behind the truck bodies, where the flow is most turbulent under the separation–convergence motion. This approach was adopted to increase the mesh density in the areas of interest and provide better resolution for the near-wall region. The side view and the cross section of the mesh generation are presented in Figures 19, 20, and 21.

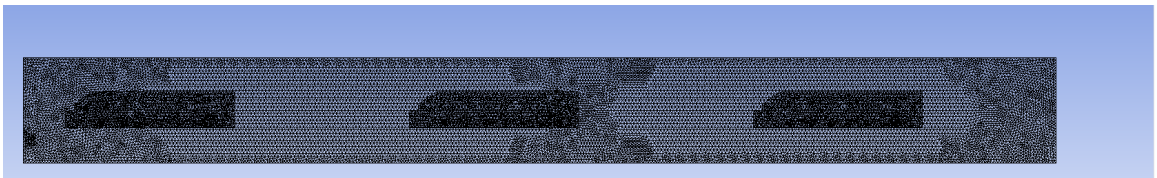

Figure 19. Diagram. Mesh generation of truck platoon, side view.

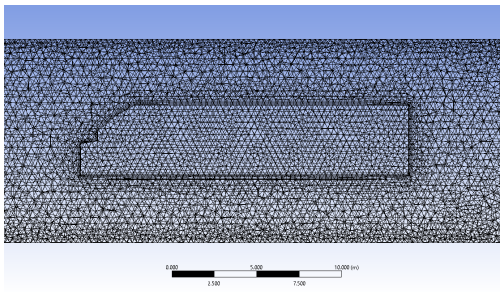

Figure 20. Diagram. Mesh generation around truck, side view.

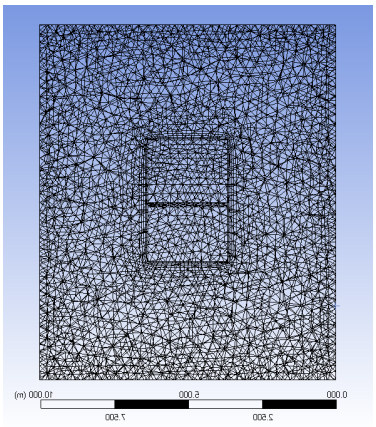

Figure 21. Diagram. Mesh generation around truck, cross-section view.

Also, it is assumed that the flow density in the computational domain is constant; and the fluid is an incompressible flow. In the domain other than the boundary layer, the fluid is considered as nonviscous fluid; and the fluid in the boundary layer around the truck surface is considered as viscous fluid. Wind speed and direction from the inlet are modified, accounting for cross-wind effects using a triangular relationship. The output parameters are drag forces and the drag coefficient for each truck.

DRAG-FORCE AND FUEL-CONSUMPTION ANALYSIS

From the CFD simulation, the drag force F_D of each truck could be estimated. Also, the drag coefficient is a dimensionless quantity that is commonly used to quantify the drag or resistance in a fluid environment. The drag coefficient c_d is defined in Equation 22:

$$c_d = \frac{2F_d}{\rho u^2 A}$$

Figure 22. Equation. Drag-coefficient calculation.

Where ρ is the air density, u is the flow speed of the truck relative to the fluid, and A is the cross-sectional area of an individual truck. Fuel-consumption rates can be investigated after obtaining the drag force of the truck-platooning system. To start with, the resistance load of the truck-platooning system is obtained in Figure 23:

$$F_{RL} = F_{Aero} + F_{RR} + F_{Grade} + F_{Iner} + F_{Cur}$$

Figure 23. Equation. Resistance load of the truck-platooning system.

Where $F_{Aero}, F_{RR}, F_{Grade}, F_{Iner}, F_{Cur}$ are aerodynamic force, rolling-resistance force, inertial force, grade resistance, and curvature resistance, respectively. The last three terms in the equation in Figure 22 are negligible when the truck-platooning system travels on a highway road with no grade and curvature impact at a constant speed. Therefore, the major source of fuel consumption of truck platooning is twofold: aerodynamics force and rolling resistance. The fuel cost, measured by monetary value per vehicle miles traveled (VMT), due to aerodynamics can be estimated by Figure 24:

$$C_{Aero}(\frac{dollar}{VMT}) = c_a \frac{1}{2} \rho A C_{\infty} v^2 R$$

Figure 24. Equation. Estimated fuel cost due to aerodynamics force.

Where c_a is a unit converting factor based on engine efficiency and diesel price, ρ is the air density, A is the cross-sectional area of an individual truck, c_{∞} is the drag coefficient of the isolated truck without platooning, v is the truck cruising speed relative to wind speed, and R is the drag-coefficient ratio of the individual truck. Furthermore, pavement roughness is one of the major factors of the rolling resistance and fuel consumption (Ziyadi et al., 2018; Okte et al., 2019; Gungor et al., 2020). The international roughness index is frequently used for measuring roadway conditions. Therefore, the roughness–speed impact model (Ziyadi et al., 2018) is adopted here to quantify the fuel consumption due to truck–pavement interaction. As shown in Figure 25, the estimated fuel cost due to pavement roughness can be expressed as a function of vehicle speed and the international roughness index:

$$C_{RSI}(\frac{dollar}{VMT}) = (\frac{p}{v} + (k_a \cdot IRI + d_a) + b \cdot v + (k_c \cdot IRI + d_c)) \times DPE \times CGD$$

Figure 25. Equation. Estimated fuel cost due to pavement roughness.

Where k_a, d_a, k_c, d_c, p, b are model coefficients for large trucks; DPE is diesel required per unit energy; CDG is the cost of diesel per gallon; and IRI is the international roughness index for highway roadway. Then, the fuel-reduction ratio Δ is defined in Figure 26:

$$\Delta = (C_{Aero} - C_{Aero,\infty})(C_{Aero,\infty} + C_{RSI})$$

Figure 26. Equation. Estimated fuel-consumption-reduction ratio.

Where $C_{Aero,\infty}$ is fuel-consumption cost due to aerodynamic drag of the isolated vehicle without the truck-platooning effect.

CHAPTER 3: DATA-DRIVEN SURROGATE MODEL FOR DRAG-FORCE PREDICTION OF A THREE-TRUCK PLATOON

The implementation of CFD simulation for various scenarios with different wind conditions and truck configurations in truck platooning is excessively time-consuming. However, quantifying the effect of wind conditions on fuel savings is crucial for optimizing truck position and achieving fuel efficiency. To overcome this limitation, in this study, a data-driven surrogate model for drag-force prediction was generated, which was used to analyze the impact of truck-platoon configurations and wind conditions on drag force and fuel reduction.

To estimate the drag force of truck platooning, different methods were implemented, including generalized additive modeling and artificial neural network. These approaches were compared with the baseline model, and the fundamentals of the generalized additive model and artificial neural network were introduced. By generating a data-driven surrogate model, the time-consuming CFD simulations were replaced with a more efficient approach, resulting in a significant reduction in computational time while still maintaining accurate predictions. This approach also provides a more comprehensive analysis of the effects of wind conditions and truck configurations on fuel savings, leading to potential optimizations in truck positioning and improved fuel efficiency.

GENERALIZED ADDITIVE MODEL

The generalized additive model (GAM) is a highly effective algorithm that offers a natural and intuitive generalization of the conventional linear model algorithms (Hastie 2017). The key feature of GAM is that it captures the relationship between the output and the interdependent input variables in a smooth and flexible manner, allowing both linear and nonlinear relationships to be modeled. GAM is designed to estimate the relationship between the output and individual input features simultaneously, with the output being estimated by adding up these relationships. This approach is highly flexible and capable of capturing complex nonlinear relationships between the output and each input feature. One of the key advantages of GAM is that it maintains a high level of interpretability, as compared to black-box neural networks. The model mathematically maps each input feature onto a nonlinear function that can be easily visualized and understood by domain experts. The GAM enables researchers to interpret and explain the results of the model in a clear and intuitive manner. The interpretability of GAM is particularly important when dealing with complex and sensitive data, where the ability to explain the model results is critical. Mathematically speaking, it maps each input feature into a nonlinear function, as shown in Figure 27:

$$g(\mathbb{E}[y_i|X_i]) = \beta_0 + f_1(x_{i1}) + f_2(x_{i2}) + \cdots + f_N(x_{iN})$$

Figure 27. Equation. Link function for the generalized additive model.

Where g is the link function that relates the predictor variables to the expected value of the dependent variable, $X_i \in \mathbb{R}^{N\times 1} = [x_{i1}, x_{i2}, \dots, x_{iN}]^T$ is the input variable, y_i is the observation of dependent variable, β_0 is the bias term, and $[f_1, f_2, \dots, f_N]$ are feature functions to automatically

model nonlinear relationships. Feature function can be chosen as an arbitrary function, which could be in parametric or nonparametric form. In this case, we choose penalized B-splines to model feature function. For each feature function, GAM uses backfitting to iteratively update the estimation f_i, as shown in Figure 28:

$$\tilde{f}_j = S(\{y_i - 1/N \sum_{p=1}^{N} y_p - \sum_{k \neq j} f_k(x_{ik})\}_{i=1}^{N})$$
$$f_j = \tilde{f}_j - 1/N \sum_{k=1}^{N} \tilde{f}_j(x_{kj}),$$

Figure 28. Equation. Iteratively backfitting in the generalized additive model.

Where S is the smoothing operator. The degree of smoothness can be estimated by maximizing the restricted maximum likelihood. For instance, for the binary GAM with a logistic link function, the restricted maximum likelihood could be expressed using Figure 29

$$L(\beta_0, f_1(x_1), \ldots, f_N(x_N)) = 2L_0(\beta_0, f_1(x_1), \ldots, f_N(x_N)) - \Sigma_{j=1}^{N} \lambda_j \int (f_j''(x_j))^2 \mathrm{d}x$$

Figure 29. Equation. Restricted-maximum-likelihood estimation.

Where $L_0(\beta_0, f_1(x_1))$ is the standard log likelihood function. The parameters $[\lambda_1, \lambda_2, \ldots, \lambda_N]$ are smoothness parameters that control the smoothness we want to impose on the model. The higher the value of the smoothness parameters, the smoother the curve.

ARTIFICIAL NEURAL NETWORK

In some complex problems, the relationship between input and output may not be easily modeled by traditional statistical techniques such as generalized linear regression or generalized additive models. In such cases, neural networks can be a powerful tool for approximating the underlying relationship between input and output.

Without loss of generality, we first introduce a single-layer neural network at layer k. Given a p-dimensional input vector $h^k \in \mathbb{R}^p$, q-dimensional, the output $h^{k+1} \in \mathbb{R}^q$ of a single-layer neural network can be expressed using Figure 30:

$$h^{k+1} = \sigma(h^k W_k + b_k)$$

Figure 30. Equation. Single layer of a fully connected network.

Where $W^k \in \mathbb{R}^{p \times q}$ and $b^k \in \mathbb{R}^{1 \times q}$ denote the weight and bias term, respectively. The function $\sigma(\cdot)$ is a nonlinear activation function. The activation function determines whether or not a neuron should

be activated by calculating the weighted sum and adding a bias term to it. The activation function introduces nonlinearity into the output of a neuron as well as the model.

The selection of activation functions plays a critical role in determining the performance of a neural network. Commonly used activation functions include sigmoid, hyperbolic tangent, rectified linear unit, and leaky rectified linear unit. In deep neural networks, the output of each activation function is transformed by a new weight matrix and a new bias term before being fed into the activation function in the next layer. The universal approximation theorem has mathematically proven that an infinity-width, single-layer neural network can approximate any continuous function $f(\cdot)$. However, due to the width limitation of neural networks and the difficulty of parameter tuning, a single-layer network is unlikely to achieve optimal performance. By stacking multiple layers, the capacity of neural networks can be readily increased, allowing improved accuracy and performance. The loss function measures the difference between the predicted and actual values, with the goal of minimizing the overall error. The use of a loss function is critical to the success of neural network models, as it allows for the optimization of model parameters to minimize the error between predicted and actual values. By carefully selecting appropriate activation functions and loss functions, neural networks can be trained to accurately model complex relationships and patterns in data. For a regression problem, a mean square error loss function in Figure 31 is typically applied to calculate the weight matrices and bias terms:

$$L(\tilde{y}, y) = \frac{1}{N}\sum_{i=1}^{N}(y_i - \tilde{y}_i)^2$$

Figure 31. Equation. Mean-square error.

Where $\tilde{y}$ and y are the prediction and the ground truth of the desired quantity, respectively; N denotes the batch size of the loss function. The optimal parameters are achieved by minimizing the loss function. Minimizing the loss function is usually performed using back-propagation. A backward pass starts from the network output and propagates toward the input layer while calculating the gradients, layer by layer, using the chain rule.

EXPERIMENT SETUP

To generate a dataset for training and testing surrogate models, we used random samples of input parameters generated from CFD simulations. The dataset was generated using Ansys with three-truck platoons. As described in Chapter 2, we generated the geometry and mesh for different truck configurations and environmental configurations. To reflect various truck-platooning scenarios, we varied the inter-truck headway from 0.1 s to 3.0 s and set the inter-truck offset from the centerline of the lane to 2ft, which kept the entire truck-platooning system in the same lane. We considered truck speeds ranging from 55 to 70 mph (88.5km/h to 112.7km/h) and maximum wind speeds of 23 mph (10.3 m/s) to cover most real-world scenarios. We used Latin hypercube sampling to generate random samples. The output of the CFD simulations was the drag force of each truck and the average drag force of the truck platooning system.

The input parameters were grouped into three categories: truck geometry, inter-truck configuration, and environmental configuration. The total number of samples generated was 16,000. We used 80% of the samples for training and 20% for testing the surrogate models. Two different surrogate models were used, including the GAM and a fully connected neural network. The GAM was fitted with linear smooth functions, an identity-link function, and a normal error distribution. The neural network was built with a five-layer, fully connected network. To optimize the model performance, the Adam optimizer (Kingma and Ba, 2014) was employed with a learning rate of 0.001. We compared the performance of the generalized additive model and neural network surrogate model to a baseline model that included linear regression (LR) and support-vector regression (SVR).

EXPERIMENT RESULT

The performance of four surrogate models was evaluated. The result comparison is presented in Table 1. The mean relative error and correlation coefficient between the predicted and CFD simulation values was used as the metric for comparison. The results demonstrate that the GAM and neural network surrogate models outperformed the LR and SVR models in terms of accuracy, with mean relative error coefficients of 4.53% and 3.27%, respectively. Additionally, the correlation coefficients between the predicted and CFD simulation values for the GAM and neural network models were 0.985 and 0.987, respectively, indicating a high level of correlation between the predicted and actual values.

Table 1. Performance Comparison of Various Surrogate Models

Model	Training Time (s)	Mean Relative Error (%)	Correlation Coefficient
Linear Regression	2.4	19.21	0.964
Support-Vector Regression	4.3	8.62	0.948
Generalized Additive Model	65.1	4.53	0.985
Neural Network	76.7	3.27	0.987

Although the training time for the GAM and neural network models was longer than that of the benchmark models, the inference time was significantly lower, at only 0.01 s per scenario. This finding suggests that the surrogate models could be used to adjust the truck configuration in real-time if the wind situation around the truck were available. Furthermore, after the surrogate model is trained, it can replace the computationally expensive CFD model and be used for drag-force prediction and fuel-consumption analysis. This change greatly reduces the computational cost and allows for faster and more efficient analysis of truck-platooning systems. Overall, the results demonstrate the effectiveness of using surrogate models for drag-force prediction and highlight their potential for real-time applications in the field of truck platooning.

CHAPTER 4: ARTIFICIAL INTELLIGENCE FOR CONNECTED-TRUCK FREIGHT DELIVERY: A CASE STUDY

Efficient connected freight operations require the consideration of several key factors, including the infrastructure required for lateral positioning, the effects of wind on truck position, and the condition of the pavement. To address this need, this study presents a virtual platoon-delivery case study that examines the performance of line-haul shipment and fuel consumption under various conditions. By evaluating the performance of the virtual platoon under various conditions, this study aims to provide valuable insights into the factors that impact the efficiency of connected freight operations.

CASE STUDY SETUP

In this study, we compared the performance of connected freight operation to traditional trucking for actual origin–destination pairs on the road network in Illinois. The selected corridor goes from a densely populated area near Chicago to a rural area in central Illinois; and we specifically focused on the route from the Amazon Fulfillment Center ORD5, located at 7001 Vollmer Road, Matteson, Illinois 60443, to Vista Outdoor, located at 1001 Innovation Road, Rantoul, Illinois 61866. To ensure accuracy, we selected the LTPP Section ID 17-5849 for our analysis.

Figure 32. Map. Map of the highway corridor in Illinois.

To evaluate the impact of platooning, as compared to normal truck traffic, we first constructed a digital twin of the actual section. Next, we considered both traditional trucking and platooning as alternatives for delivering parcels between the two points. Finally, we compared these two alternatives to quantify the costs and benefits of platooning, taking into account factors such as operation, reliability, and energy reduction. Our aim was to provide valuable insights into the potential benefits of platooning in real-world, freight-delivery scenarios, and to demonstrate the practicality and effectiveness of this approach in reducing transportation costs and enhancing energy efficiency. Figure 32 provides a detailed view of the corridor under consideration.

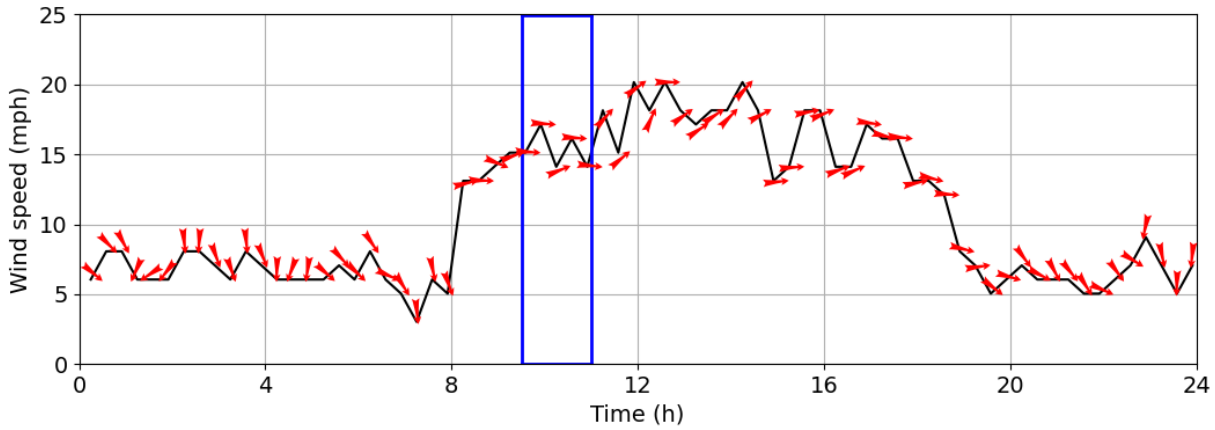

Figure 33. Graph. Wind history along the highway corridor.

The case study involved a truck freight-delivery scenario in March 2022. The wind speed and direction data were collected from the wind stations located in Rantoul and in Kankakee, which is near the corridor. The wind resolution was set at 20 min, and the wind speed and direction were assumed to be constant during each 20-min interval. The corridor selected for the study is 100 mi long, offering high platoonability. For simplicity in the case study, the delivery corridor is assumed to be a straight line. The total delivery time was set at 1.5 hr, and a delivery window is from 10 am to 11.30 am. The wind history along the highway segment is depicted in Figure 33, with wind speeds fluctuating between 6 m/s (13.4 mph) and 8 m/s (18 mph), and wind direction changing from WNW to WSW. This information set the basis for the study and provided crucial insights into the environmental conditions that affect the performance of the platoon. Figure 34 indicates the average drag force under different headways; the headways used in the three figures are 0.18 s, 0.57 s, and 2.5 s. The average drag force was found to increase with headway, which means fuel consumption increases if headway increases. Furthermore, the changes in lateral offset (δ1 = truck 1-2 and δ2 = truck 2-3 offset) also contribute to the average drag force. To illustrate, for each headway, the average drag force decreases when the offset of trucks 2 and 3 are similar, δ1 = δ2. It indicates that the trailing truck is benefiting from the low-pressure zone created by the middle truck. In addition, differences in optimal lateral offsets under different headway scenarios were negligible.

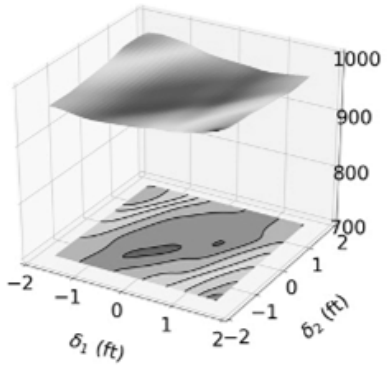

A. Headway = 0.18 s

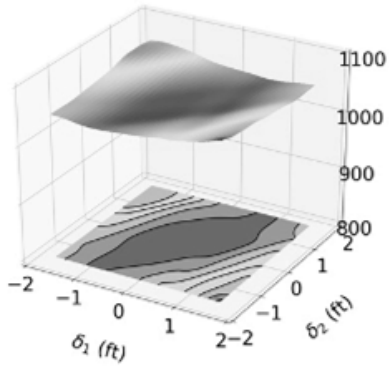

B. Headway = 0.57 s

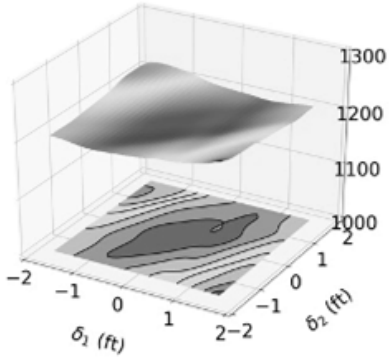

C. Headway = 2.5 s

Figure 34. Graphs. Average drag-force prediction under various headways

The fuel-reduction ratio calculated using the equation in Figure 25 for three-truck platoons is presented in Figure 35. The middle truck and trailing truck used less fuel than the lead truck. Accounting for the communication, controller, and mechanical latency, a time gap greater than 0.5 s is typical. For three-truck platoons running at a speed of 122.65 km/h (70 mph), fuel reduction would be 7% and 3% at a time gap of 0.57 s and 2.5 s, respectively. With the development of V2V and CACC,

if the communication latency between trucks could be reduced (< 0.5 s), fuel reduction may approach 10%.

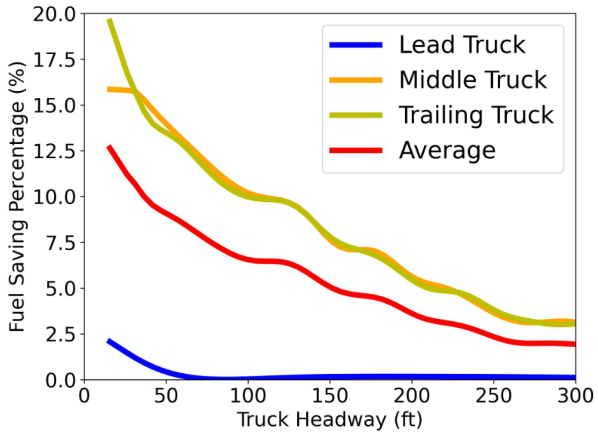

Figure 35. Graph. Fuel-consumption-reduction ratio for a three-truck platoon.

Line-haul delivery cost for the truck-platoon system is threefold: (1) fuel consumption, (2) operation cost and labor cost, and (3) vehicle depreciation and overhead cost. The labor-cost rate and overhead-cost rate are assumed to be $60/truck-hr and $25/truck-hr, respectively. It is also assumed that a total of 1,000 parcels are delivered from the origin to the destination. Furthermore, drivers will be required in all trucks under conventional truck-delivery conditions, but a driver is required in only the lead truck under the fully automated platooning condition, which reduces the operational cost due to labor and driver salary. The fuel consumption of heavy-duty trucks is calculated using the equations in Figures 23 and 24, respectively. The operational cost was estimated for serving the same set of demands using a three-truck-platoon system and a nonplatooning delivery system. As presented in Figure 36, the cost due to fuel consumption and cost due to labor and truck depreciation are both reduced due to truck-platoon automation. And the total cost of the line-haul delivery with fully automated truck platooning is highly reduced, from $0.83 per parcel to $0.61 per parcel, about 26%.

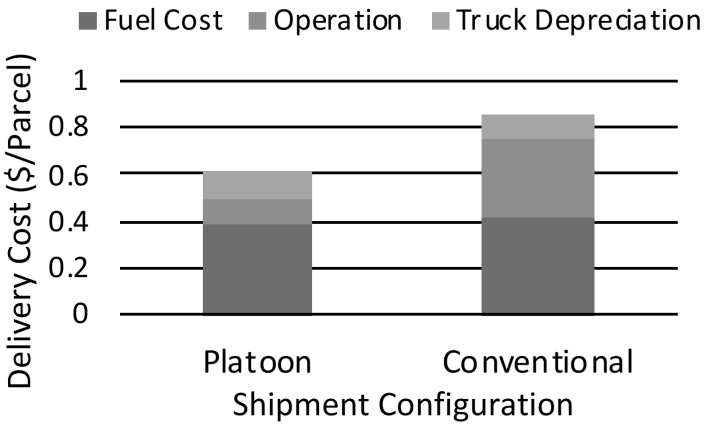

Figure 36. Graph. Delivery-cost comparison between three-truck platoon and nonplatoon.

SUMMARY

The advancements in autonomous and connected truck technologies bring drastic changes in freight delivery. One of the most notable changes is the formation of truck platoons. Vehicle-to-vehicle and vehicle-to-infrastructure communication has become a reality with the help of autonomous and connected trucks. Despite the numerous benefits of truck platooning, this approach requires a significant amount of computational resources to obtain aerodynamic performance. To overcome this challenge, a data-driven surrogate model for drag-force prediction was developed using the generalized additive model and artificial neural network to predict the average drag force accurately and efficiently for any given wind condition. Compared with the baseline result of linear regression, the prediction error between the surrogate model and CFD simulation is reduced to 3.27%. The average fuel-consumption-reduction ratio could be up to 10% and 7% for truck spacings of 5.5 m (18 ft) and 19.8 m (65 ft), respectively.

As a case study, the cost–benefit analysis of parcel-delivery and fuel-consumption analysis of a three-truck platoon in Illinois on the I-57 highway is examined. The total cost of the line-haul delivery with fully automated truck platooning is highly reduced, from $0.83 per parcel to $0.61 per parcel, about 26%. This difference highlights the importance of truck platooning as a solution for reducing fuel consumption and improving delivery economy in the freight industry.

REFERENCES

ANSYS, Inc. (2016) ANSYS Fluent User's Guide, Release 17.2.

Bounini, F., Gingras, D., Lapointe, V., & Pollart, H. (2015). "Autonomous vehicle and real time road lanes detection and tracking." In *2015 IEEE Vehicle Power and Propulsion Conference (VPPC)* (pp. 1–6). IEEE. https://doi.org/10.1109/VPPC.2015.7352903

Browand, F., McArthur, J., & Radovich, C. (2004). "Fuel saving achieved in the field test of two tandem trucks." Research Report. UC Berkeley: California Partners for Advanced Transportation Technology. https://escholarship.org/uc/item/29v570mm

Dar, K., Bakhouya, M., Gaber, J., Wack, M., & Lorenz, P. (2010). "Wireless communication technologies for ITS applications" [Topics in Automotive Networking]. *IEEE Communications Magazine,* 48(5), 156–162. https://doi.org/10.1109/MCOM.2010.5458377

Gidel, S., Checchin, P., Blanc, C., Chateau, T., & Trassoudaine, L. (2010). "Pedestrian detection and tracking in an urban environment using a multilayer laser scanner." *IEEE Transactions on Intelligent Transportation Systems, 11*(3), 579–588. https://doi.org/10.1109/TITS.2010.2045122

Gong, X., Gu, Z., Li, Z., Song, X., & Wang, Y. (2010). *Aerodynamic Shape Optimization of a Container-Truck's Wind Deflector Using Approximate Model* (No. 2010-01-2035). SAE Technical Paper. SAE International. https://doi.org/10.4271/2010-01-2035

Gungor, O. E., She, R., Al-Qadi, I. L., & Ouyang, Y. (2020). "One for all: Decentralized optimization of lateral position of autonomous trucks in a platoon to improve roadway infrastructure sustainability*." Transportation Research Part C: Emerging Technologies,* 120, 102783. https://doi.org/10.1016/j.trc.2020.102783

Hastie, T. J. (2017). "Generalized additive models." In *Statistical models in S* (pp. 249–307). Routledge.

Ho, G. T. S., Tsang, Y. P., Wu, C. H., Wong, W. H., & Choy, K. L. (2019). "A computer vision-based roadside occupation surveillance system for intelligent transport in smart cities." *Sensors, 19*(8), 1796. https://doi.org/10.3390/s19081796

Humphreys, H., & Bevly, D. (2016). *Computational fluid dynamic analysis of a generic 2 truck platoon (No. 2016-01-8008).* SAE Technical Paper. SAE International. https://doi.org/10.4271/2016-01-8008

Hussein, A. A., & Rakha, H. A. (2021). "Vehicle platooning impact on drag coefficients and energy/fuel saving implications." *IEEE Transactions on Vehicular Technology, 71*(2), 1199–1208. https://doi.org/10.1109/TVT.2021.3131305

Iowa State University. (July 28, 2023). IEM Site Information. Iowa Environmental Mesonet. https://mesonet.agron.iastate.edu/sites/locate.php

Katreddi, S., & Thiruvengadam, A. (2021). "Trip based modeling of fuel consumption in modern heavy-duty vehicles using artificial intelligence." *Energies, 14*(24), 8592. https://doi.org/10.3390/en14248592

Khan, J. F., Bhuiyan, S. M., & Adhami, R. R. (2010). "Image segmentation and shape analysis for road-

sign detection." *IEEE Transactions on Intelligent Transportation Systems, 12*(1), 83–96. https://doi.org/10.1109/TITS.2010.2073466

Khurana, S., Saxena, S., Jain, S., & Dixit, A. (2021). "Predictive modeling of engine emissions using machine learning: A review." In *Materials Today: Proceedings, 38* (pp. 280–284). https://doi.org/10.1016/j.matpr.2020.07.204

Kingma, D. P., & Ba, J. (2014). "Adam: A method for stochastic optimization." *arXiv* preprint *arXiv:*1412.6980. https://doi.org/10.48550/arXiv.1412.6980

Liu, T., & Meidani, H. (2023). "Optimizing Seismic Retrofit of Bridges: Integrating Efficient Graph Neural Network Surrogates and Transportation Equity." In *Proceedings of Cyber-Physical Systems and Internet of Things Week 2023* (pp. 367–372). https://doi.org/10.1145/3576914.3587503

Liu, T., & Meidani, H. (2022). "Graph Neural Network Surrogate for seismic reliability analysis of highway bridge system." *arXiv* preprint. *arXiv:*2210.06404. https://doi.org/10.48550/arXiv.2210.06404

Liu, W., Muramatsu, S., & Okubo, Y. (2018). "Cooperation of V2I/P2I communication and roadside radar perception for the safety of vulnerable road users." In *2018 16th International Conference on Intelligent Transportation Systems Telecommunications (ITST)* (pp. 1–7). IEEE. https://doi.org/10.1109/ITST.2018.8566704

Liu, Y., & Moser, A. (2003). "Numerical modeling of airflow over the Ahmed body." Eleventh annual conference of the CFD Society of Canada (CFD 2003) Proceedings, (pp. 507-512). Canada: CFD Society of Canada.

Lu, X. Y., & Shladover, S. E. (2014). "Automated truck platoon control and field test." *Road Vehicle Automation,* 247–261. https://doi.org/10.1007/978-3-319-05990-7_21

Mak, S., Sung, C. L., Wang, X., Yeh, S. T., Chang, Y. H., Joseph, V. R., Yang, V., & Wu, C. J. (2018). "An efficient surrogate model for emulation and physics extraction of large eddy simulations." *Journal of the American Statistical Association, 113*(524), 1443–1456. https://doi.org/10.1080/01621459.2017.1409123

McAuliffe, B., Croken, M., Ahmadi-Baloutaki, M., & Raeesi, A. (2017). "Fuel-economy testing of a three-vehicle truck platooning system." Research Report. University of California, Berkeley. https://escholarship.org/uc/item/7g37w4fb

McAuliffe, B. R., & Ahmadi-Baloutaki, M. (2018). "A wind-tunnel investigation of the influence of separation distance, lateral stagger, and trailer configuration on the drag-reduction potential of a two-truck platoon." *SAE International Journal of Commercial Vehicles, 11*(2), 125–150.

Müller, S. (2012) "The Impact of Electronic Coupled Heavy Trucks on Traffic Flow." In *ETC Proceedings.* 40th European Transport Conference (ECT), 8–10 October 2012, Glasgow.

Okte, E., Al-Qadi, I. L., & Ozer, H. (2019). "Effects of pavement condition on LCCA user costs." *Transportation Research Record: Journal of the Transportation Research Board, 2673*(5), 339–350. https://doi.org/10.1177/0361198119836776

Pustokhina, I.V., Pustokhin, D.A., Rodrigues, J.J., Gupta, D., Khanna, A., Shankar, K., Seo, C., & Joshi,

G.P. (2020). “Automatic vehicle license plate recognition using optimal K-means with convolutional neural network for intelligent transportation systems.” *IEEE Access, 8,* 92907–92917. https://doi.org/10.1109/ACCESS.2020.2993008

Schleicher, D., Bergasa, L. M., Ocaña, M., Barea, R., & López, M. E. (2009). “Real-time hierarchical outdoor SLAM based on stereovision and GPS fusion.” *IEEE Transactions on Intelligent Transportation Systems, 10*(3), 440–452. https://doi.org/10.1109/TITS.2009.2026317

Schroten, A., Warringa, G., & Bles, M. (2012). “Marginal abatement cost curves for heavy duty vehicles.” Background report. Delft, CE Delft. https://cedelft.eu/publications/marginal-abatement-cost-curves-for-heavy-duty-vehicles/

Teter, J., Cazzola, P., Gul, T., Mulholland, E., Le Feuvre, P., Bennett, S., Hugues, P., Lagarde, Z., Kraayvanger, V., Bryant, T., & Scheffer, S. (2017). *The future of trucks: Implications for energy and the environment.* International Energy Agency, Paris. (167 pp.). https://doi.org/10.1787/9789264279452-en

Tsugawa, S. (2014). “Results and issues of an automated truck platoon within the energy ITS project.” In *2014 IEEE Intelligent Vehicles Symposium Proceedings* (pp. 642–647). IEEE. https://doi.org/10.1109/IVS.2014.6856400

Van der Pol, E., & Oliehoek, F. A. (2016). “Coordinated deep reinforcement learners for traffic light control.” In *Proceedings of learning, inference and control of multi-agent systems (at NIPS 2016), 8* (pp. 21–38).

Vegendla, P., Sofu, T., Saha, R., Kumar, M. M., & Hwang, L. K. (2015). *Investigation of aerodynamic influence on truck platooning* (No. 2015-01-2895). SAE Technical Paper. SAE International. https://doi.org/10.4271/2015-01-2895

Wan, X., Lucic, M. C., Ghazzai, H., & Massoud, Y. (2020). “Empowering real-time traffic reporting systems with nlp-processed social media data.” *IEEE Open Journal of Intelligent Transportation Systems, 1,* 159–175. https://doi.org/10.1109/OJITS.2020.3024245

Zhang, J., Tan, B., Sha, F., & He, L. (2011a). “Predicting pedestrian counts in crowded scenes with rich and high-dimensional features.” *IEEE Transactions on Intelligent Transportation Systems, 12*(4), 1037–1046. https://doi.org/10.1109/TITS.2011.2132759

Zhang, J., Wang, F. Y., Wang, K., Lin, W. H., Xu, X., & Chen, C. (2011b). “Data-driven intelligent transportation systems: A survey.” *IEEE Transactions on Intelligent Transportation Systems, 12*(4), 1624–1639. https://doi.org/10.1109/TITS.2011.2158001

Zhao, D., Qin, H., Song, B., Zhang, Y., Du, X., & Guizani, M. (2020). “A reinforcement learning method for joint mode selection and power adaptation in the V2V communication network in 5G.” *IEEE Transactions on Cognitive Communications and Networking, 6*(2), 452–463. https://doi.org/10.1109/TCCN.2020.2983170

Ziyadi, M., Ozer, H., Kang, S., & Al-Qadi, I. L. (2018). “Vehicle energy consumption and an environmental impact calculation model for the transportation infrastructure systems.” *Journal of Cleaner Production, 174,* 424–436. https://doi.org/10.1016/j.jclepro.2017.10.292